

# 1 Security and Communication Networks

## 2 Secure Information Transmissions in Wireless-powered Cognitive

### 3 Radio Networks for Internet of Medical Things

4 K. Tang,<sup>1,3</sup> W. Tang,<sup>2</sup> E. Luo,<sup>3</sup> Z. Tan<sup>4</sup>, W. Meng<sup>5</sup>, L. Qi<sup>6</sup>

5 <sup>1</sup> Guangdong Provincial Key Laboratory of Millimeter-Wave and Terahertz, School of  
6 Electronic and Information Engineering, South China University of Technology, Guangzhou  
7 510641, China.

8 <sup>2</sup> College of Computer Science and Electronic Engineering, Hunan University, Changsha  
9 410082, China.

10 <sup>3</sup> School of Electronics and Information Engineering, Hunan University of Science and  
11 Engineering, Yongzhou 425000, China.

12 <sup>4</sup> School of Computing, Edinburgh Napier University, Edinburgh EH11 4BN, United Kingdom.

13 <sup>5</sup> Department of Applied Mathematics and Computer Science, Technical University of  
14 Denmark, Lyngby 2800 Kgs., Denmark.

15 <sup>6</sup> School of Information Science and Engineering, Qufu Normal University, Rizhao 276826,  
16 China.

17 Correspondence should be addressed to E. Luo; [luoentao\\_huse@163.com](mailto:luoentao_huse@163.com)

18

## 19 Abstract

20 In this paper, we consider the issue of the secure transmissions for the cognitive radio-based  
21 Internet of Medical Things (IoMT) with wireless energy harvesting. In these systems, a primary  
22 transmitter (PT) will transmit its sensitive medical information to a primary receiver (PR) by a  
23 multi-antenna-based secondary transmitter (ST), where we consider that a potential  
24 eavesdropper may listen the PT's sensitive information. In the meanwhile, the ST also  
25 transmits its own information concurrently by utilizing spectrum sharing. We aim to propose a  
26 novel scheme for jointly designing the optimal parameters, i.e., energy harvesting (EH) time  
27 ratio and secure beamforming vectors, for maximizing the primary secrecy transmission rate  
28 while guaranteeing secondary transmission requirement. For solving the non-convex  
29 optimization problem, we transfer the problem into convex optimization form by adopting the  
30 semi-definite relaxation (SDR) method and Charnes-Cooper transformation technique. Then,  
31 the optimal secure beamforming vectors and energy harvesting duration can be obtain easily  
32 by utilizing the CVX tools. According to the simulation results of secrecy transmission rate,  
33 i.e., secrecy capacity, we can observe that the proposed protocol for the considered system  
34 model can effectively promote the primary secrecy transmission rate when compared with

35 traditional zero-forcing (ZF) scheme, while ensuring the transmission rate of the secondary  
36 system.

## 37 **I. Introduction**

38 With the rapid development of wireless communication and networking technologies, an  
39 increasing number of devices need to be connected globally and communicate automatically.  
40 Therefore, the emerging of the Internet of Things (IoT) as a promising paradigm can achieve a  
41 fusing of the various technologies in 5G communication systems, which have been widely  
42 applied in smart cities, agriculture, and environment monitoring [1-6]. Moreover, the medical  
43 care and health care have becoming one of the most popular applications based on the IoT [7,8],  
44 named the Internet of Medical Things (IoMT), which can collect the data from the medical  
45 devices and applications to improve the treatment effect, disease diagnosis, and patient  
46 experience, while reduce decrease misdiagnosis rate and treatment cost. According to the  
47 investigation of relevant organizations, the market share of IoMT will reach to roughly 117  
48 billion dollars by the end of 2020 [9]. However, with the increasing use of IoMT equipment,  
49 the huge demand for radio spectrum has become a serious problem. In addition, the allocated  
50 radio spectrums are often underutilized due to the inflexible spectrum policies [10]. In order to  
51 facilitate an effective utilization of spectrum resources, cognitive radio technology was  
52 introduced in which unlicensed nodes could communicate with each other in an opportunistic  
53 manner over a licensed frequency band without interrupting the primary transmissions [11-13].

54 Yet, power supply is another key constraint on the development of IoMT. In general, an IoMT  
55 system usually contains a large number of small-size devices that are battery-powered and  
56 difficult to be replaced. In order to solve this problem, wireless-powered technology has been  
57 paid high attention. The devices with EH capabilities can convert energy from the surrounding  
58 environment into electricity for data transmission, such as solar, wind, or RF signals [14].  
59 Especially with the synchronous development of antenna and circuit designs, wireless EH  
60 based on RF signals has attracted more attention due to its advantages of wireless, low cost and  
61 small form implementation [15-17]. Furthermore, the amount of harvested energy is in  
62 milliwatts, which is enough to power small-size IoMT devices, such as medical data sensors  
63 for short-distance transmissions. Therefore, the combination of cognitive radio and EH in  
64 medical wireless sensor networks can greatly improve both the spectrum and energy  
65 efficiencies.

66 Although adopting cognitive radio technology with EH can effectively improve the transfer  
67 efficiency for IoMT, the variety of medical devices in healthcare fields will introduce several  
68 security problems [18]. Since the energy-constraint sensors need to perform energy harvesting  
69 and then forward the sensitive patient data wirelessly, the other illegal sensors may be the  
70 potential eavesdropper to listen such confidential messages [19]. As an emerging field, a large  
71 number of healthcare manufacturers are rushing to utilize the IoT solutions in some  
72 applications without considering security. As a result, there will bring new security problems  
73 related to confidentiality, integrity, and availability. Furthermore, due to the limited capabilities,  
74 such as lack of effective computation and sufficient power supply, many sensors in IoMT  
75 cannot embed encryption algorithm. Therefore, these lack of strong encryption across medical  
76 sensors make themselves to be discovered and exploited by malicious users easily.

## 77 A. Related work

78 To take the full advantage of the potential gains for wireless EH, the researchers developed  
 79 simultaneous wireless information and power transmission (SWIPT) schemes in wireless  
 80 networks that utilize RF signals to transmit energy and information to receivers. Authors in  
 81 [20] applied the SWPIT in relay interference channels for multiple source-destination pairs  
 82 communication system, where each pair of link has a dedicated EH relay serving for relaying  
 83 transmission. On this basis, the optimal power allocation ratio for each relay was deduced by  
 84 adopting the distributed power allocation framework of game theory. A SWIPT scheme for  
 85 amplify-and-forward (AF) bidirectional relaying network based on OFDM was proposed in  
 86 [21], where a wireless-powered relay performed information processing and EH by utilizing  
 87 two disjoint subcarriers groups, respectively. Based on the decode-and-forward (DF) mode, the  
 88 authors in [22] designed an optimal resource allocation strategy to maximize the energy  
 89 efficiency with non-linear SWIPT model under a two-way relay network. For cognitive radio  
 90 networks with energy harvesting in IoT systems, the authors in [23] analyzed the outage  
 91 probability of a random underlay cognitive network with EH-based assistant relay. The two  
 92 main challenges for cognitive radio sensor networks in IoT systems were considered in [24],  
 93 where the authors developed an architecture and proposed an energy management strategy for  
 94 achieving balance between the transmission performance of the networks and operational life.  
 95 In [25], the authors considered the insecure characteristic of electronic medical records based  
 96 on eHealth systems, and then proposed a corresponding secure encrypted scheme to ensure the  
 97 data security. In [26], the authors investigated an overlaid spectrum sharing network with  
 98 SWIPT for IoT systems, where a pair of SWIPT-based devices as the relays to assist the  
 99 transmission of the primary signals. Considering information security in cognitive radio-based  
 100 IoT systems, the authors in [27] presented a novel algorithm for channel allocation with time-  
 101 sensitive data under the scenario of jamming attacks. A secure relay selection scheme based on  
 102 channel state information and battery state information was proposed for energy harvesting-  
 103 based cognitive radio networks in IoT networks [28].

## 104 B. Motivation and Contributions

105 Unlike the mentioned literates [27] and [28] in above, we consider an actual application  
 106 scenarios for sanatorium or hospital under the cognitive radio-based IoTM networks to protect  
 107 the patients' sensitive medical information. Considering an indoor environment for sanatorium  
 108 or hospital, where the PT intends to transmit its sensitive medical data to the PR, while the ST  
 109 performs data monitoring and transfer to the SR. In this scenario, the node ST has lack of  
 110 energy supply and need to scavenge energy from the primary transmitter, while ST can be  
 111 regarded as the relay to opportunistically access the licensed primary channel. Meanwhile, we  
 112 assume that an attacker is located near the PR to eavesdrop the PT's medical data. Thus, to  
 113 enable the secure transmission of the PT's signal, we investigate a typical cognitive radio  
 114 network with wireless-powered relay (CRN-WPR) and jointly design the optimal EH time ratio  
 115 and secure beamforming vectors to maximize the secrecy transmission rate of the primary  
 116 system, while effectively guarantee the secondary transmission rate. The main contributions  
 117 are summarized as follows:

- 118 • We propose a corresponding protocol for EH and secrecy information transmission for a  
 119 cognitive radio-based IoMT system, where the relay node ST is equipped with multiple-  
 120 antenna to perform EH at first and then transfers the sensitively primary signal with DF  
 121 processing to the destination in security with its own signal.

- 122 • In order to protect the sensitive medical data sending from the PT, we formulate the  
 123 optimization problem based on maximizing the secrecy transmission rate of the primary  
 124 system while ensuring the transmission requirement of the secondary system. We adopt  
 125 SDR and Charnes-Cooper transformation to transform the non-convex optimization  
 126 problem into a convex optimization problem to find a solution for the optimization  
 127 problem. A corresponding algorithm is then developed. In addition, the zero-forcing (ZF)  
 128 scheme is also applied to solve the optimization problem as a benchmark.
- 129 • The numerical results of the influence for the secrecy transmission rate on the primary  
 130 system under different system parameters are given, such as primary transmission power,  
 131 number of antennas, and transmission distance, etc. The results demonstrate excellent  
 132 secure transmission performance with proposed scheme than ZF scheme.

133 The rest of this paper is organized as follows. The section II introduces the system model and  
 134 transmission protocol. Section III formulates the optimization problem and proposes the  
 135 corresponding solution with secure beamforming. Furthermore, the ZF scheme is also adopted  
 136 to solve the optimization as a benchmark. The section IV presents the simulation results and  
 137 corresponding analyses. The section V summarizes this paper.

138 *Notations:* Throughout this paper, let  $(\cdot)^H$  denote the conjugate transpose.  $\mathbf{I}$  presents the identity matrix with  
 139 appropriate dimension.  $[x]^+$  represents the maximum value between  $x$  and 0, while  $x^*$  denotes the optimal  
 140 value of  $x$ .  $\Pi_x^\perp$  denotes the orthogonal projection onto the orthogonal complement of the column space of  $x$ .  
 141  $\|\cdot\|$  denotes the Euclidean norm of a vector or a matrix and  $|\cdot|$  denotes the magnitude of a channel or the absolute  
 142 value of a complex number. Table I lists the fundamental notations and parameters.

143  
 144

Table 1: List of parameters and their physical meaning/expression.

Parameter	Meaning/Expression
$\mathbf{h}_{PST}, \mathbf{h}_{SS}, \mathbf{h}_{SME}, \mathbf{h}_{SPR}$	$N \times 1$ complex channel vectors of the PT-ST, ST-SR, ST-ME, and ST-PR, respectively
$h_{PP}, h_{PME}$	Channel coefficients of the PT-PR and the PT-ME
$\alpha$	Duration of energy harvesting
$T$	Total block time
$x_e, x_p$	Transmit dedicated energy signal and confidential signal at PT
$\hat{x}_p, x_s$	Decoded primary signal and secondary signal at ST
$P_p$	PT's transmission power
$\mathbf{n}_{ST}, n_{PR}, n_{ME}, n_{SR}$	Received AWGN at ST, PR, ME, and SR
$\eta$	Energy conversion efficiency from signal power to circuit power
$R_{ST}, R_{PR}, R_{ME}, R_{SR}$	Achievable rate at ST, PR, ME, and SR, respectively
$\tilde{R}_{PR}, \tilde{R}_{ME}$	Overall transmission rates at PR and ME
$R_{SEC}$	Secrecy rate of the primary system
$\mathbf{v}_p, \mathbf{v}_s$	Relaying beamforming vector and cognitive beamforming vector
$E_{ST0}$	Initial power at the ST
$r_s$	Minimal transmission rate requirement for the secondary system

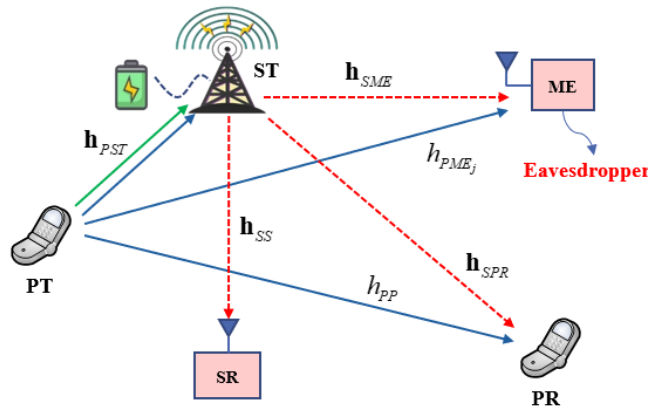
$\Gamma$	An auxiliary optimization variable to bound the achievable rate of the eavesdropper ME
$\beta$	Power allocation coefficient

## 145 II. System Model and Transmission Protocol

### 146 A. System Model

147 We consider a cognitive radio network with wireless-powered relay (CRN-WPR) as shown in  
 148 Fig. 1. The primary system is composed of a primary transmitter (PT) and a primary receiver  
 149 (PR), while the secondary system consists of a secondary transmitter (ST) and a secondary  
 150 receiver (SR). There also exists an eavesdropper (ME) whose purpose is to intercept the PT's  
 151 confidential data in the range of the primary system, where PT intends to send a confidential  
 152 data to PR. The primary system may be regard as the uplink of the transmission system with  
 153 poor channel quality or lower rate. Therefore, the ST is willing to act as the relay for assisting  
 154 the primary transmission while delivering its own data. We assume that the PT has a fixed  
 155 power supply, while the ST may have limited battery storage, so it needs to obtain energy from  
 156 the received RF signal. The ST is equipped with  $N$  antennas and other nodes operates in half-  
 157 duplex mode with single antenna.

158 All channels undergo the flat block Rayleigh fading channel, which is characterized by quasi-  
 159 static state of the channel in one transmission-slot and independent change in different  
 160 transmission-slots. Let  $\mathbf{h}_{PST}$ ,  $\mathbf{h}_{SS}$ ,  $\mathbf{h}_{SME}$ , and  $\mathbf{h}_{SPR}$  be the  $N \times 1$  complex channel vectors of the  
 161 PT-ST, ST-SR, ST-ME, and ST-PR, respectively. The channel coefficients of the PT-PR and  
 162 the PT-ME links are denoted by  $h_{PP}$  and  $h_{PME}$ . The global channel state information is  
 163 available for the system, which is a common assumption in physical-layer security literatures  
 164 [29,30].



165

166 Figure 1: System model of a CRN-WPR. The green line denotes the first phase for energy harvesting, the blue  
 167 lines and red lines represent the second and third information transmission phases from the PT and ST,  
 168 respectively.

### 169 B. Energy Harvesting and Information Transmission

170 As depicted in Fig. 1, the EH and information transmission in one transmission-slot includes  
 171 three phases. In the first phase, the PT uses a portion of time  $\alpha$  ( $\alpha \in (0,1)$ ) of the total block

172 time  $T$  to transmit the dedicated energy signal  $x_e$  to ST for EH. Thus, the received signal at the  
173 ST can be expressed as

$$174 \quad y_{ST}^I = \sqrt{P_p} \mathbf{h}_{PST} x_e + \mathbf{n}_{ST}, \quad (1)$$

175 where  $P_p$  represents the transmission power of the node PT,  $x_e$  denotes the unit-power energy  
176 signal,  $\mathbf{n}_{ST} \sim \mathcal{CN}(0, \delta_{ST} \mathbf{I})$  is the received additive Gaussian white noise (AWGN) with  
177 variance of  $\delta_{ST}$ . For definiteness and without loss of generality, we assume  $T=1$ . Thus, the  
178 amount of harvested energy at the ST can be calculated as

$$179 \quad E_{ST} = \alpha \eta P_p \|\mathbf{h}_{PST}\|^2, \quad (2)$$

180 where  $\eta \in [0,1]$  is energy conversion efficiency. Note that the amount of scavenged energy  
181 from noise is neglected because the harvested energy from the thermal noise can be negligible  
182 compared to the energy signal.

183 At the second phase of duration  $(1-\alpha)T/2$ , the PT transmits confidential signal  $x_p$  with  
184 power  $P_p$ , the received signal at the ST is thus given as

$$185 \quad y_{ST}^{II} = \sqrt{P_p} \mathbf{h}_{PST} x_p + \mathbf{n}_{ST}. \quad (3)$$

186 The achievable rate  $R_{ST}$  can be derived as

$$187 \quad R_{ST} = \frac{(1-\alpha)T}{2} \log_2 \left( 1 + \frac{P_p \|\mathbf{h}_{PST}\|^2}{\delta_{ST}} \right). \quad (4)$$

188 Due to the nature of the information broadcast, the PR and eavesdropper ME can also receive  
189 the signal  $x_p$ , the received signals at the PR and ME are given as

$$190 \quad \begin{aligned} y_{PR}^{II} &= \sqrt{P_p} h_{PP} x_p + n_{PR}, \\ y_{ME}^{II} &= \sqrt{P_p} h_{PME} x_p + n_{ME}, \end{aligned} \quad (5)$$

191 respectively. Here,  $n_{PR} \sim \mathcal{CN}(0, \delta_{PR})$  and  $n_{ME} \sim \mathcal{CN}(0, \delta_{ME})$  denote AWGN at PR and ME,  
192 respectively.

193 During the third phase  $(1-\alpha)T/2$ , the node ST first decodes the received primary confidential  
194 signal  $\hat{x}_p$  based on DF processing, and then simultaneously forwards  $\hat{x}_p$  and its own signal  
195  $x_s$  by utilizing the beamforming vectors  $\mathbf{v}_p \in \mathbb{C}^{N \times 1}$  and  $\mathbf{v}_s \in \mathbb{C}^{N \times 1}$ , respectively. Therefore,  
196 the corresponding received signal at the PR and eavesdropper ME are expressed as

$$\begin{aligned}
197 \quad y_{PR}^{\text{III}} &= \mathbf{h}_{SPR}^H \mathbf{v}_P \hat{x}_P + \mathbf{h}_{SPR}^H \mathbf{v}_S x_S + \mathbf{n}_{PR}, \\
y_{ME}^{\text{III}} &= \mathbf{h}_{SME}^H \mathbf{v}_P \hat{x}_P + \mathbf{h}_{SME}^H \mathbf{v}_S x_S + \mathbf{n}_{PR},
\end{aligned} \tag{6}$$

198 respectively. The PR attempts to retrieve  $\hat{x}_p$  from  $y_{PR}^{\text{III}}$  in the presence of the secondary signal  
199  $x_s$ . In the meanwhile, the eavesdropper also intends to intercept signal  $\hat{x}_p$ . Thus, the  
200 achievable rates at the PR and ME in last two phases can be expressed as

$$\begin{aligned}
201 \quad R_{PR} &= \frac{(1-\alpha)T}{2} \log_2 \left( 1 + \frac{P_P |h_{PP}|^2}{\delta_{PR}} + \frac{|\mathbf{h}_{SPR}^H \mathbf{v}_P|^2}{|\mathbf{h}_{SPR}^H \mathbf{v}_S|^2 + \delta_{PR}} \right), \\
R_{ME} &= \frac{(1-\alpha)T}{2} \log_2 \left( 1 + \frac{P_P |h_{PME}|^2}{\delta_{ME}} + \frac{|\mathbf{h}_{SME}^H \mathbf{v}_P|^2}{|\mathbf{h}_{SME}^H \mathbf{v}_S|^2 + \delta_{ME}} \right).
\end{aligned} \tag{7}$$

202 At the SR, the received signal is given by

$$203 \quad y_{SR} = \mathbf{h}_{SS}^H \mathbf{v}_S x_S + \mathbf{h}_{SS}^H \mathbf{v}_P \hat{x}_P + \mathbf{n}_{SR}. \tag{8}$$

204 Similar to the PR, the SR treats  $\hat{x}_p$  as interference and then detects the desired secondary signal  
205  $x_s$ . The achievable rate at the SR is given by

$$206 \quad R_{SR} = \frac{(1-\alpha)T}{2} \log_2 \left( 1 + \frac{|\mathbf{h}_{SS}^H \mathbf{v}_S|^2}{|\mathbf{h}_{SS}^H \mathbf{v}_P|^2 + \delta_{SR}} \right). \tag{9}$$

### 207 III. Problem Formulation and Secure Beamforming

208 In this section, we first define the secrecy rate of the primary system, which is a critical  
209 performance index to illustrate the transmission security of the sensitive data [31, 32], and then  
210 formulate the optimization problem with maximizing the primary secrecy rate aiming to satisfy  
211 the minimum achievable rate for the secondary system and power constraint of the relay node  
212 ST. In order to effectively obtain the optimal parameters to keep data in safety, we also propose  
213 a mathematically efficient optimization scheme to solve the problem with two-stage procedure.

#### 214 A. Problem Formulation

215 Based on the DF cooperative communication scheme, the overall transmission rates at PR and  
216 ME equal to the minimum rate of the two-hop transmissions, respectively [32], i.e.,

$$\begin{aligned}
217 \quad \tilde{R}_{PR} &= \min \{ R_{ST}, R_{PR} \}, \\
\tilde{R}_{ME} &= \min \{ R_{ST}, R_{ME} \}.
\end{aligned} \tag{10}$$

218 Based on the definition of [33], the secrecy rate of the primary system for the considered  
219 secrecy CRN-WPR can be expressed as

220 
$$R_{SEC} = \left[ \tilde{R}_{PR} - \tilde{R}_{ME} \right]^+ . \quad (11)$$

221 Substituting the results of Equation (8) into Equation (9), the overall primary secrecy rate is  
222 then given as

223 
$$R_{SEC} = \left[ \min \{ R_{ST}, R_{PR} \} - R_{ME} \right]^+ . \quad (12)$$

224 In the following, the EH ratio and secure beamforming vectors are jointly designed by  
225 maximizing the primary secrecy rate subject to the minimum achievable rate for the SR and  
226 power constraint of the ST. Mathematically, the considered optimization problem can be  
227 represent as (P1):

$$\begin{aligned} & \max_{\alpha, \mathbf{v}_P, \mathbf{v}_S} \left[ \min \{ R_{ST}, R_{PR} \} - R_{ME} \right]^+ \\ & s.t. \\ & \text{C1: } R_{SR} \geq r_s, \\ & \text{C2: } \|\mathbf{v}_P\|^2 + \|\mathbf{v}_S\|^2 \leq \frac{2(\alpha\eta P_P \|\mathbf{h}_{PST}\|^2 + E_{ST0})}{1-\alpha}, \\ & \text{C3: } 0 < \alpha < 1. \end{aligned} \quad (13)$$

228

229 In (13), C1 means that the achievable rate of SR should be larger than or equal to minimum  
230 rate  $r_s$ . C2 denotes the transmission power constraint at the ST with  $E_{ST0}$  representing the  
231 initial power at the ST.

## 232 B. Optimal Secure Beamforming Design

233 According to the analysis of formula (13), we can observe that (P1) is a non-convex function,  
234 which is difficult to derive three optimal variables  $(\alpha, \mathbf{v}_P, \mathbf{v}_S)$  concurrently. In the followings,  
235 this section proposes a mathematically efficient optimization scheme with two-stage procedure  
236 for solving the (P1):

- 237 • In the stage I, we obtain the optimal secure beamforming  $(\mathbf{v}_P^*, \mathbf{v}_S^*)$  for any given energy  
238 harvesting duration  $\alpha$  ;  
239 • In the stage II, the global optimal solution  $(\alpha^*, \mathbf{v}_P^*, \mathbf{v}_S^*)$  can be found based on one-  
240 dimension search over  $\alpha$  .

241 In the stage I, the maximization of the primary secrecy rate is equivalent to maximizing the  
242 achievable rate of the PR subject to an alternative upper bound on the achievable rate of ME.  
243 Thus, for a given  $\alpha = \alpha_0$ ,  $R_{ST}(\alpha_0)$  is the constant value and the problem (P1) can be  
244 transformed into follows problem (P2):

$$\max_{\mathbf{v}_P, \mathbf{v}_S} \frac{(1-\alpha_0)T}{2} \log_2 \left( 1 + \frac{P_P |h_{PP}|^2}{\delta_{PR}} + \frac{|\mathbf{h}_{SPR}^H \mathbf{v}_P|^2}{|\mathbf{h}_{SPR}^H \mathbf{v}_S|^2 + \delta_{PR}} \right)$$

s.t.

245

$$\text{C1: } \frac{(1-\alpha_0)T}{2} \log_2 \left( 1 + \frac{|\mathbf{h}_{SS}^H \mathbf{v}_S|^2}{|\mathbf{h}_{SS}^H \mathbf{v}_P|^2 + \delta_{SR}} \right) \geq r_S, \quad (14)$$

$$\text{C2: } \|\mathbf{v}_P\|^2 + \|\mathbf{v}_S\|^2 \leq \frac{2(\alpha_0 \eta P_P \|\mathbf{h}_{PST}\|^2 + E_{ST0})}{1-\alpha_0},$$

$$\text{C3: } \frac{(1-\alpha_0)T}{2} \log_2 \left( 1 + \frac{P_P |h_{PME}|^2}{\delta_{ME}} + \frac{|\mathbf{h}_{SME}^H \mathbf{v}_P|^2}{|\mathbf{h}_{SME}^H \mathbf{v}_S|^2 + \delta_{ME}} \right) \leq \Gamma,$$

246  
247  
248  
249  
250

where  $\Gamma$  represents an auxiliary optimization variable to bound the achievable rate of the eavesdropper ME, thus the maximum primary secure rate can be obtained by adjusting value of  $\Gamma$ . The optimal value of  $\Gamma^*$  can be founded by one-dimension search since it is a non-negative value. Note that the optimization problem (P2) is still non-convex concerning with beamforming vectors  $\mathbf{v}_P$  and  $\mathbf{v}_S$ .

251  
252  
253  
254  
255  
256  
257

Considering  $\log_2(x)$  is monotonically increasing function of  $x$  and defining  $\mathbf{H}_{SPR} = h_{SPR} h_{SPR}^H$ ,  $\mathbf{H}_{SME} = h_{SME} h_{SME}^H$ ,  $\mathbf{H}_{SS} = h_{SS} h_{SS}^H$ ,  $\mathbf{V}_P = \mathbf{v}_P \mathbf{v}_P^H$ , and  $\mathbf{V}_S = \mathbf{v}_S \mathbf{v}_S^H$ , the problem (P2) can be denoted as a fractional programming problem, but the objective function is still non-convex since two optimization variables  $\mathbf{V}_P$  and  $\mathbf{V}_S$  are existed in numerator and denominator of objective function, respectively. To solve the problem (P2) more effectively, the fractional programming problem can be equivalently reformulated to a convex SDR problem by utilizing Charnes-Cooper transformation [34]. Thus, we let

258

$$\lambda = \frac{1}{\text{tr}(\mathbf{H}_{SPR} \mathbf{V}_S) + \delta_{SR}}, \quad (15)$$

259  
260

while defining  $\tilde{\mathbf{V}}_P = \lambda \mathbf{V}_P$  and  $\tilde{\mathbf{V}}_S = \lambda \mathbf{V}_S$ , the corresponding SDR of problem (P2) can be rewritten as (P3)

$$\begin{aligned}
& \max_{\mathbf{v}_P, \mathbf{v}_S, \lambda} \text{tr}(\mathbf{H}_{SPR} \tilde{\mathbf{V}}_P) \\
& \text{s.t.} \\
& \text{C1: } \text{tr}(\mathbf{H}_{SPR} \tilde{\mathbf{V}}_S) + \lambda \delta_{SR} = 1, \\
& \text{C2: } \text{tr}(\mathbf{H}_{SS} \tilde{\mathbf{V}}_S) - \Gamma_S \text{tr}(\mathbf{H}_{SS} \tilde{\mathbf{V}}_P) \geq \lambda \Gamma_S \delta_{SR}, \\
& \text{C3: } \text{tr}(\tilde{\mathbf{V}}_P) + \text{tr}(\tilde{\mathbf{V}}_S) \leq \frac{2\lambda(\alpha_0 \eta P_P \|\mathbf{h}_{PST}\|^2 + E_{ST0})}{1 - \alpha_0} \\
& \text{C4: } \text{tr}(\mathbf{H}_{SME} \tilde{\mathbf{V}}_P) - \Gamma_e \text{tr}(\mathbf{H}_{SME} \tilde{\mathbf{V}}_S) \leq \lambda \Gamma_e \delta_{ME}, \\
& \text{C5: } \tilde{\mathbf{V}}_P \succeq 0, \tilde{\mathbf{V}}_S \succeq 0, \lambda > 0,
\end{aligned} \tag{16}$$

$$\text{where } \Gamma_S = 2^{\frac{2r_S}{1-\alpha_0}} - 1 \text{ and } \Gamma_e = 2^{\frac{2\Gamma}{1-\alpha_0}} - \frac{P_P |h_{PME}|^2}{\delta_{ME}} - 1.$$

It must be noted that SDR cannot guarantee to derive the optimal solution  $(\mathbf{v}_P^*, \mathbf{v}_S^*)$  with rank-one. In the followings, the first step is to prove that the rank of optimal  $\tilde{\mathbf{V}}_P^*$  equals to one, then we propose a method to structure the optimal  $\tilde{\mathbf{V}}_S^*$  with rank-one when the rank of  $\tilde{\mathbf{V}}_S$  is greater than one.

Let  $\theta_1, \theta_2, \theta_3$ , and  $\theta_4$  represents the Lagrange multipliers, i.e., dual variables, related to constraints C1 to C4 in Equation (16), respectively. Thus, the corresponding Lagrange function of problem (P3) can be expressed as

$$\mathcal{L}(\tilde{\mathbf{V}}_P, \tilde{\mathbf{V}}_S, \theta_1, \theta_2, \theta_3, \theta_4) = \text{tr}(\xi \tilde{\mathbf{V}}_P) + \text{tr}(\psi \tilde{\mathbf{V}}_S) + \rho, \tag{17}$$

where

$$\xi = \mathbf{H}_{SPR} - \theta_2 \Gamma_S \mathbf{H}_{SS} - \theta_3 \mathbf{I} - \theta_4 \mathbf{H}_{SME}, \tag{18}$$

$$\psi = -\theta_1 \mathbf{H}_{SPR} + \theta_2 \mathbf{H}_{SS} - \theta_3 \mathbf{I} + \theta_4 \Gamma_e \mathbf{H}_{SME}, \tag{19}$$

and  $\rho$  denotes the residual information that is not related for the proof. According to the definition of Karush-Kuhn-Tucker conditions and Lagrange function of problem (P3), we thus have

$$\xi^* \tilde{\mathbf{V}}_P^* = 0, \psi^* \tilde{\mathbf{V}}_S^* = 0. \tag{20}$$

Assuming the harvested energy and initial energy are all used for secure beamforming transmission in the third phase, the power constraint C3 in Equation (16) is activated with equality, thus the dual variable  $\theta_3^* > 0$ . Since the transmission channel vectors  $\mathbf{H}_{SS} \succeq 0$  and  $\mathbf{H}_{SME} \succeq 0$ , we can derive that  $\text{rank}(-\theta_2^* \Gamma_S \mathbf{H}_{SS} - \theta_3^* \mathbf{I} - \theta_4^* \mathbf{H}_{SME}) = N$ . Furthermore, since

282  $\text{rank}(\mathbf{H}_{SPR}) \leq 1$ , it follows that  $\text{rank}(\xi^*) \geq N-1$ . Based on Equation (20), we thus obtain  
 283  $\text{rank}(\tilde{\mathbf{V}}_P^*) = 1$ .

284 Define  $\kappa^* = -\theta_1^* \mathbf{H}_{SPR} - \theta_2^* \mathbf{H}_{SS} - \theta_3^* \mathbf{I} + \theta_4^* \mathbf{H}_{SME}$ , thus we have

$$285 \quad \psi^* = \kappa^* + 2\theta_2^* \mathbf{H}_{SS}. \quad (21)$$

286 Since  $\mathbf{H}_{SPR} \succeq 0$ ,  $\mathbf{H}_{SS} \succeq 0$ , and  $\mathbf{H}_{SME} \succeq 0$ , we can obtain that  
 287  $\text{rank}(-\theta_1^* \mathbf{H}_{SPR} - \theta_2^* \mathbf{H}_{SS} - \theta_3^* \mathbf{I}) = N$ . Moreover, since  $\text{rank}(\mathbf{H}_{SME}) \leq 1$ , it can be derived that  
 288  $\text{rank}(\kappa^*) \geq N-1$ .

- 289 • If  $\text{rank}(\kappa^*) = N$ , we can obtain that  $\text{rank}(\psi^*) = N-1$ , thus it follows from Equation (20)  
 290 that  $\text{rank}(\tilde{\mathbf{V}}_S^*) = 1$  and  $\tilde{\mathbf{V}}_S^*$  is equal to  $aww^H$ , where  $w \in \mathbb{C}^{N \times 1}$  denotes the spanning null  
 291 space of  $\psi^*$  and  $a > 0$ . Thus, the corresponding optimal value of (P3) is  $(\tilde{\mathbf{V}}_P^*/\lambda^*, \tilde{\mathbf{V}}_S^*/\lambda^*)$ ;
- 292 • If  $\text{rank}(\kappa^*) = N-1$ , we can observe that  $\text{rank}(\tilde{\mathbf{V}}_S^*) > 1$  and thus it requires constructing a  
 293 new solution with rank-one. First, we obtain the orthonormal basis  $u \in \mathbb{C}^{N \times 1}$  of the null  
 294 base of  $\kappa^*$ , which is defined as  $\kappa^* u = 0$  and  $\text{rank}(u) = 1$ . Then, based on the expression of  
 295  $\kappa^*$ , we can further derive that  $\mathbf{H}_{SS} u = 0$ . Thus, the optimal solution of  $\tilde{\mathbf{V}}_S^*$  is given by

$$296 \quad \tilde{\mathbf{V}}_S^* = buu^H + aww^H, \quad (22)$$

298 where  $b \geq 0$ ,  $\|w\| = 1$ , and  $w^H u = 0$ . Finally, the optimal result of  $\hat{\mathbf{V}}_S^*$  with rank-one can be  
 299 rewritten as  $\hat{\mathbf{V}}_S^* = \tilde{\mathbf{V}}_S^* - buu^H$ . Thus, the reconstructed optimal solution for (P3) is  
 300  $(\tilde{\mathbf{V}}_P^*/\lambda^*, \hat{\mathbf{V}}_S^*/\lambda^*)$ .

301 For fixed  $\alpha = \alpha_0$ , the optimal solutions  $(\Gamma^*, \tilde{\mathbf{V}}_P^*, \tilde{\mathbf{V}}_S^*)$  can be obtained through one-dimension  
 302 search  $\Gamma$  based on the following equation

$$303 \quad (\Gamma^*, \mathbf{V}_P^*, \mathbf{V}_S^*) = \arg \max_{\alpha = \alpha_0} \text{problem(P3)}, \quad (23)$$

304 thus the optimal secure beamforming vectors  $(\mathbf{v}_P^*, \mathbf{v}_S^*)$  can be obtained by adopting  
 305 eigenvalue decomposition (EVD) of  $\tilde{\mathbf{V}}_P^*/\lambda^*$  and  $\tilde{\mathbf{V}}_S^*/\lambda^*$ .

306 In order to obtain the global optimal solution for problem (P1) in the second stage, one-  
 307 dimension search related to  $\alpha$  is then utilized. The optimal solution is chosen from the  
 308 following equation

$$309 \quad (\alpha^*, \Gamma^*, \mathbf{v}_P^*, \mathbf{v}_S^*) = \arg \max_{\alpha \in (0,1)} \text{problem(P1)}. \quad (24)$$

310 The whole algorithm process can be described as follows:

---

**Algorithm 1** Optimal Secure Beamforming Design

---

**Initialize**  $\alpha=\alpha_0$  and  $\Gamma=\Gamma_0$ ; Define  $\Gamma_{\max}$  as a large positive real number,  $\Delta\alpha$  and  $\Delta\tau$  are all small positive real numbers as the iterative steps for one-dimension search.

1: **for** a given  $\alpha=\alpha_0$  **do** S1-S4

2: S1: Given  $\Gamma=\Gamma_0$ , then solve problem (P3) and derive the optimal solution  $(\tilde{\mathbf{V}}_p^*, \tilde{\mathbf{V}}_s^*, \lambda^*)$  by utilizing CVX tools;

3: S2: Obtain optimal  $(\tilde{\mathbf{V}}_p^*, \tilde{\mathbf{V}}_s^*)$  through the following procedures;

4: **if**  $\text{rank}(\tilde{\mathbf{V}}_p^*)=1$  and  $\text{rank}(\tilde{\mathbf{V}}_s^*)=1$ , **then**

5: The optimal solution for problem (P3) is  $(\tilde{\mathbf{V}}_p^*/\lambda^*, \tilde{\mathbf{V}}_s^*/\lambda^*)$ ;

6: **else**

7: Reconstruct an optimal solution  $(\tilde{\mathbf{V}}_p^*/\lambda^*, \hat{\mathbf{V}}_s^*/\lambda^*)$  for problem (P3) with  $\text{rank}(\tilde{\mathbf{V}}_p^*)=1$  and  $\text{rank}(\hat{\mathbf{V}}_s^*)=1$  based on Equation (22);

8: **end if**

9: S3: **Let**  $\Gamma=\Gamma+\Delta\tau$  when  $\Gamma < \Gamma_{\max}$  and then go to S1-S2;

10: S4: **Choose** the optimal solution  $(\Gamma^*, \mathbf{V}_p^*, \mathbf{V}_s^*)$  from Equation (23) and derive optimal secure beamforming vectors  $(\mathbf{v}_p^*, \mathbf{v}_s^*)$  by performing EVD.

11: **end for**

12: **Update**  $\alpha=\alpha+\Delta\alpha$  and S1-S4;

**Choose** the optimal solution  $(\alpha^*, \Gamma^*, \mathbf{v}_p^*, \mathbf{v}_s^*)$  based on Equation (24).

---

### 311 C. Secure Beamforming based on Zero-forcing Rule

312 This section investigates another secure beamforming solution based on Zero-forcing (ZF)  
 313 rule as a benchmark, which the primary transmission will not be interfered by other  
 314 transmissions. Therefore, based on the criterion of ZF rule [35], the beamforming vectors  
 315  $\mathbf{v}_{s,ZF}$  and  $\mathbf{v}_{p,ZF}$  for the primary and secondary systems should be in the null space of  $\mathbf{h}_{SPR}^\perp$   
 316 and  $\mathbf{h}_{SS}^\perp$ , respectively, i.e.,  $\mathbf{h}_{SPR}^H \mathbf{v}_{s,ZF} = 0$  and  $\mathbf{h}_{SS}^H \mathbf{v}_{p,ZF} = 0$ . Since there exists an  
 317 eavesdropper in the system to listen the primary's confidential information, so that the  
 318 beamforming  $\mathbf{v}_{p,ZF}$  should also be in the null space of  $\mathbf{h}_{SME}^\perp$ , i.e.,  $\mathbf{h}_{SME}^H \mathbf{v}_{p,ZF} = 0$ . In order to  
 319 be fair in secondary transmission power, we further define  $\mathbf{v}_{p,ZF} = \sqrt{\beta P_{ST}} \hat{\mathbf{v}}_{p,ZF}$  and  
 320  $\mathbf{v}_{s,ZF} = \sqrt{(1-\beta) P_{ST}} \hat{\mathbf{v}}_{s,ZF}$  with  $\hat{\mathbf{v}}_{p,ZF}^H \hat{\mathbf{v}}_{p,ZF} = 1$  and  $\hat{\mathbf{v}}_{s,ZF}^H \hat{\mathbf{v}}_{s,ZF} = 1$ , where  $\beta$  represents the

321 power allocation coefficient and  $P_{ST} = 2\left(\alpha\eta P_P \|\mathbf{h}_{PST}\|^2 + E_{ST0}\right)/(1-\alpha)$  denotes the secondary  
 322 transmission power. Based on Equations (13) and (14), the optimization problem based on ZF  
 323 rule can be formulated as (P4):

$$\begin{aligned}
 & \max_{\hat{\mathbf{v}}_{P,ZF}, \hat{\mathbf{v}}_{S,ZF}} \frac{(1-\alpha)T}{2} \log_2 \left( 1 + \frac{P_P |h_{PP}|^2 + \beta P_{ST} |\mathbf{h}_{SPR}^H \hat{\mathbf{v}}_{P,ZF}|^2}{\delta_{PR}} \right) \\
 & \text{s.t.} \\
 & \text{C1: } \frac{(1-\alpha)T}{2} \log_2 \left( 1 + \frac{(1-\beta)P_{ST} |\mathbf{h}_{SS}^H \hat{\mathbf{v}}_{S,ZF}|^2}{\delta_{SR}} \right) \geq r_S, \\
 & \text{C2: } \frac{(1-\alpha)T}{2} \log_2 \left( 1 + \frac{P_P |h_{PME}|^2}{\delta_{ME}} \right) \leq \Gamma, \\
 & \text{C3: } \mathbf{h}_{SPR}^H \hat{\mathbf{v}}_{S,ZF} = 0, \mathbf{h}_{SS}^H \hat{\mathbf{v}}_{P,ZF} = 0, \mathbf{h}_{SME}^H \hat{\mathbf{v}}_{P,ZF} = 0, \\
 & \text{C4: } 0 < \alpha < 1.
 \end{aligned} \tag{25}$$

325 Based on the objective function of the optimization problem (P4), we can observe that the  
 326 optimal  $\hat{\mathbf{v}}_{P,ZF}$  should maximize the primary transmission rate under the constraint C3. Thus,  
 327 the optimal  $\mathbf{v}_{P,ZF}$  can be obtained by utilizing the following optimization problem:

$$\begin{aligned}
 & \max_{\mathbf{v}_{P,ZF}} |\mathbf{h}_{SPR}^H \hat{\mathbf{v}}_{P,ZF}|^2 \\
 & \text{s.t. } \mathbf{h}_{SS}^H \hat{\mathbf{v}}_{P,ZF} = 0, \mathbf{h}_{SME}^H \hat{\mathbf{v}}_{P,ZF} = 0,
 \end{aligned} \tag{26}$$

329 Since both the constraint functions in Equation (26) include  $\hat{\mathbf{v}}_{P,ZF}$ , we thus can define a new  
 330 matrix  $\mathbf{H}_S = [\mathbf{h}_{SS}^H; \mathbf{h}_{SME}^H]$  and the constraint function can be rewritten as  $\mathbf{H}_S \hat{\mathbf{v}}_{P,ZF} = 0$ . To  
 331 satisfy the new constraint,  $\hat{\mathbf{v}}_{P,ZF}$  can be obtained by solving the orthogonal value of  $\mathbf{H}_S$ ,  
 332 which means that  $\hat{\mathbf{v}}_{P,ZF}$  should be the null space of  $\mathbf{H}_S$ . To obtain the maximization of  
 333  $|\mathbf{h}_{SPR}^H \hat{\mathbf{v}}_{P,ZF}|^2$ , the optimal  $\hat{\mathbf{v}}_{P,ZF}^*$  should be chosen the one which is in the direction of the  
 334 orthogonal projection of  $\mathbf{h}_{SPR}^H$  on to the subspace  $\mathbf{H}_S^\perp$ , where the optimal  $\hat{\mathbf{v}}_{P,ZF}^*$  is given by

$$\hat{\mathbf{v}}_{P,ZF}^* = \frac{\left( \mathbf{I} - \frac{\mathbf{H}_S \mathbf{H}_S^H}{\|\mathbf{H}_S\|^2} \right) \mathbf{h}_{SPR}}{\left\| \left( \mathbf{I} - \frac{\mathbf{H}_S \mathbf{H}_S^H}{\|\mathbf{H}_S\|^2} \right) \mathbf{h}_{SPR} \right\|}. \tag{27}$$

336 Similarly, the optimal  $\hat{\mathbf{v}}_{S,ZF}^*$  can be derived by analyzing the constraint function  
 337  $\mathbf{h}_{SPR}^H \hat{\mathbf{v}}_{S,ZF} = 0$  in Equation (25), where the  $\hat{\mathbf{v}}_{S,ZF}^*$  should be the null space of  $\mathbf{h}_{SPR}^H$ , i.e.,  $\hat{\mathbf{v}}_{S,ZF}^*$

338 belongs to the subspace  $\mathbf{h}_{SPR}^\perp$ . Here, we try to maximize the  $|\mathbf{h}_{SS}^H \hat{\mathbf{v}}_{S,ZF}|^2$  so that more ST's  
 339 transmission power can be used to transfer primary data to effectively ensure the secure  
 340 transmission of information in the primary system. Therefore, the optimal  $\hat{\mathbf{v}}_{S,ZF}^*$  can be  
 341 derived as

$$342 \quad \hat{\mathbf{v}}_{S,ZF}^* = \frac{\left( \mathbf{I} - \frac{\mathbf{h}_{SPR} \mathbf{h}_{SPR}^H}{\|\mathbf{h}_{SPR}\|^2} \right) \mathbf{h}_{SS}}{\left\| \left( \mathbf{I} - \frac{\mathbf{h}_{SPR} \mathbf{h}_{SPR}^H}{\|\mathbf{h}_{SPR}\|^2} \right) \mathbf{h}_{SS} \right\|}. \quad (28)$$

343 According to (25), we can find that the objective function is an increasing function while C1  
 344 is a decreasing function with the increase of  $\beta$ , we can obtain the optimal  $\beta^*$  through  
 345 deriving the upper-bound of  $\beta$ . Therefore, the optimal  $\beta^*$  can be expressed as

$$346 \quad \beta^* = 1 - \delta_{SR} \left( \frac{2^{\frac{2r_s}{(1-\alpha)T}} - 1}{P_{ST} |\mathbf{h}_{SS}^H \hat{\mathbf{v}}_{S,ZF}^*|^2} \right). \quad (29)$$

347 Then, the optimal energy harvesting duration  $\alpha^*$  and  $\Gamma^*$  can be derived by adopting one-  
 348 dimension search.

#### 349 IV. Simulations and Analyses of Security Transmission Performance

350 In this section, we will verify security transmission performance of the primary and  
 351 transmission efficiency of secondary system by comparing the proposed scheme and ZF-based  
 352 scheme. Unless stated otherwise, we assume that all noise power are normalized to unity, i.e.,  
 353  $\delta_{PR} = \delta_{SR} = \delta_{ME} = 1$ . We also consider a scenario where the transmission distance between the  
 354 PT and PR is 8 m, while the distance between the ST and SR is 3 m. Moreover, the ST is  
 355 equipped with 4 antennas and the energy harvesting efficiency is set as  $\eta=0.5$ . The

356 transmission channel can be modeled as  $h = d^{-\frac{\varpi}{2}} e^{j\omega}$  with  $d$  and  $\varpi=3.5$  denoting the distance  
 357 and path loss exponent, respectively [36]. The minimum transmission rate of the secondary  
 358 system and maximal auxiliary optimization variable are set to be  $r_s=0.5$  bit/s/Hz and  
 359  $\Gamma_{\max}=1.0$  bit/s/Hz, respectively.

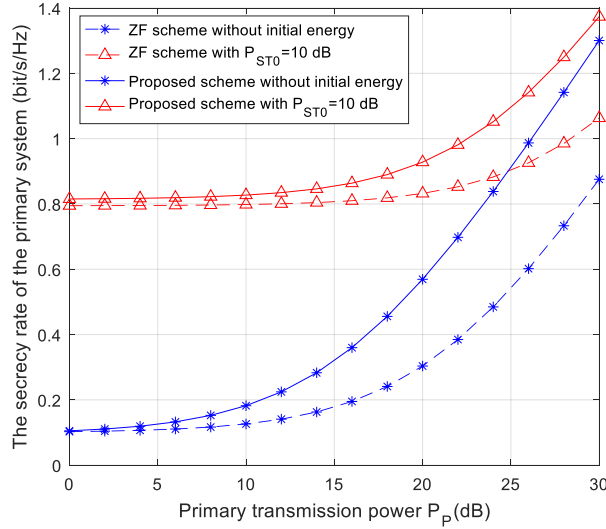


Figure 2: The secrecy rate of the primary system with respect to the primary transmission power  $P_p$  for different initial energy at the ST. The antenna number  $N=4$ ,  $d_{PST}=4$  m,  $d_{SPR}=d_{PP}-d_{PST}$ ,  $d_{PME}=d_{PP}$ .

Figure 2 illustrates the secrecy rate of the primary system with respect to the primary transmission power for different initial energy at the ST. In this figure, both the secrecy rates of the primary system with proposed scheme and ZF scheme are improved with the increase of primary transmission power, respectively. Moreover, the proposed scheme outperforms the ZF scheme in terms of the primary's secrecy rate. With the lower primary transmission power, the superiority of the proposed scheme is obviously and the primary secrecy rates with both schemes are close in high primary transmission power. With the increase of the initial energy at the ST, the secrecy rate gets better as shown in Figure 2 since the more transmission power will be utilized to assist the transmission of the primary signals.

Figure 3 compares the secrecy rates of the primary system with proposed scheme and ZF scheme against the antenna number at the ST. Obviously, with the increase of the antenna number, the secrecy rates gets better continually since more antenna will result in a higher spatial reuse efficiency. Similarly, the primary secrecy rate is always high for the proposed scheme.

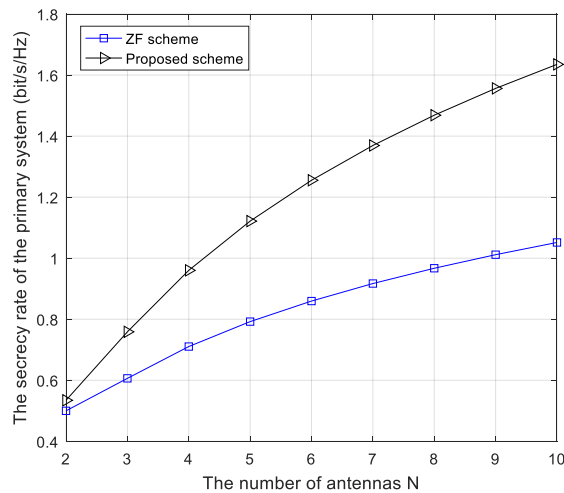


Figure 3: The secrecy rate of the primary system with respect to the number of antenna at the ST.  $P_p=10$ dB,  $P_{ST0}=0$ dB.  $d_{PST}=4$  m,  $d_{SS}=2$  m,  $d_{SPR}=d_{PP}-d_{PST}$ ,  $d_{SME}=d_{SPR}$ ,  $d_{PME}=d_{PP}$ .

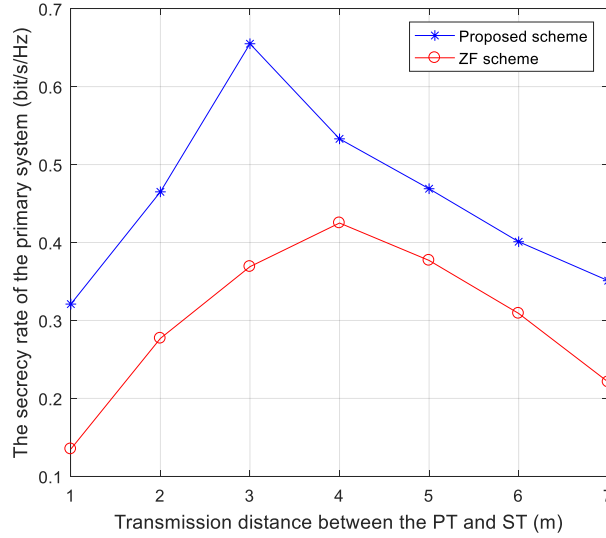


Figure 4: The secrecy rate of the primary system with respect to the distance between the PT and ST.  $P_p=10\text{dB}$ ,  $P_{ST0}=0\text{dB}$ ,  $d_{SS}=2\text{ m}$ ,  $d_{SPR}=d_{PP}-d_{PST}$ ,  $d_{SME}=d_{SPR}$ ,  $d_{PME}=d_{PP}$ . The antenna number  $N=4$ .

Figure 4 shows the primary secrecy rates with the proposed scheme and ZF scheme against the transmission distance between the PT and ST. From this figure, we can observe that the proposed scheme is superiority to the ZF scheme in term of the primary secrecy rate, regardless the position of the ST. With the increase of the  $d_{PST}$ , the primary secrecy rates first become better and then become worse. When the transmission distance  $d_{PST}$  is short, the secrecy rates get better with the increase of the  $d_{PST}$  because the more energy will be harvested for signal transmission and shorter distance for primary signal transferring. However, when the distance  $d_{PST}$  is longer, the secrecy rates get worse since the amount of harvested energy will be decreased and more path-loss will result in a negative effect for the ST to process the PT's signal. Furthermore, we can obtain that the optimal positions of the ST are roughly 3m and 4m for the proposed scheme and ZF scheme, respectively.

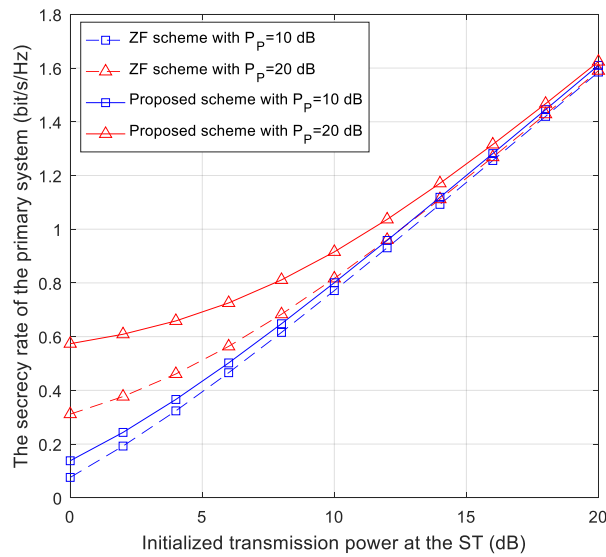
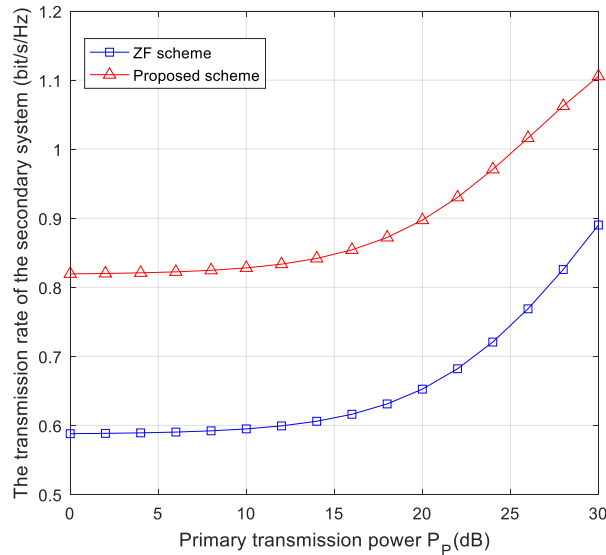


Figure 5: The secrecy rate of the primary system with respect to the initialized transmission power  $P_{ST0}$  at the ST for different primary transmission power  $P_p$ .  $d_{PST}=4\text{ m}$ ,  $d_{SS}=2\text{ m}$ ,  $d_{SPR}=d_{PP}-d_{PST}$ ,  $d_{SME}=d_{SPR}$ ,  $d_{PME}=d_{PP}$ . The antenna number  $N=4$ .

404 The Figure 5 shows the secrecy rate of the primary system corresponding to the ST's initial  
 405 energy for different primary transmission power. In this figure, we can observe that the secrecy  
 406 rates of the primary system with both the schemes are close with the increase of the ST's initial  
 407 energy, which further illustrates the proposed scheme is superior to the ZF scheme. Specifically,  
 408 the proposed scheme outperforms the ZF scheme in a lower primary power range. However,  
 409 in the higher initial primary power range, the gap of the secrecy rates of the primary system  
 410 between the proposed scheme and the ZF scheme gets small. Therefore, the proposed scheme  
 411 in this paper is more effective when the initial energy is small.



412 Figure 6: The transmission rate of the secondary system with respect to the primary transmission power  $P_p$ .  
 413  $P_{ST0}=10\text{dB}$ .  $d_{PST}=4\text{ m}$ ,  $d_{SS}=2\text{ m}$ ,  $d_{SPR}=d_{PP}-d_{PST}$ ,  $d_{SME}=d_{SPR}$ ,  $d_{PME}=d_{PP}$ . The antenna number  $N=4$ .

414  
415

416 Figure 6 shows the achievable rate of the secondary system with respect to the primary  
 417 transmission power. From the figure, the throughput of the secondary system with both the  
 418 scheme are enhanced with the increase of the primary transmission power, which because of  
 419 more energy will be harvested for the signal transmission. In the meanwhile, the propose  
 420 scheme outperforms the ZF scheme, which verifies the effectiveness of the proposed scheme.

## 421 V. Conclusions

422 This paper studied the secure transmission problem for the cognitive radio-based IoMT with  
 423 energy harvesting when the sensitive medical data send from the PT can be listened by a  
 424 malicious eavesdropper. For the sake of protecting the security of the sensitive data, we formula  
 425 the corresponding optimization problem and propose a novel algorithm for jointly designing  
 426 optimal EH duration and secure beamforming vectors to maximizing the primary secrecy  
 427 transmission rate while ensuring the transmission requirement of the secondary system. In fact,  
 428 the number of eavesdroppers may usually more than one, the proposed scheme still can be  
 429 utilized to obtain optimized beamforming vectors. The numerical results presents excellent  
 430 secure transmission performance with proposed scheme than zero-forcing scheme, which can  
 431 be implemented into the IoMT devices to effectively protect the security of the sensitive data.

## 432 Conflicts of Interest

433 The authors declare that there is no conflict of interest regarding the publication of this paper.

## 434 **Funding Statement**

435 The authors thank the Research Foundation of China Postdoctoral Science Foundation under  
 436 Grant No.2019M652895, in part by the Research Foundation of Education Department of Hunan  
 437 Province under Grant No.18B517, and in part by the Teaching Reform Research Project of  
 438 Hunan University of Science and Engineering under Grant No.XKYJ2018023, and in part by  
 439 the Construct Program of Applied Characteristic Discipline in Hunan University of Science  
 440 and Engineering.

## 441 **Acknowledgements**

442 Not applicable

## 443 **References**

- 444 [1] C. Zhu, V.C.M. Leung, L. Shu, et al., “Green Internet of Things for smart world,” *IEEE Access*, vol. 3,  
 445 pp. 2151–2162, 2015.
- 446 [2] K. Zhang, J. Ni, K. Yang, et al., “Security and privacy for smart city applications: Challenges and  
 447 solutions,” *IEEE Communications Magazine*, vol. 55, no. 1, pp. 122–129, 2017.
- 448 [3] J. Ni, K. Zhang, X. Lin, et al., “Securing fog computing for Internet of Things applications: Challenges  
 449 and solutions,” *IEEE Communications Surveys & Tutorials*, vol. 20, no. 1, pp. 601–628, 2018.
- 450 [4] F. Montori, L. Bedogni, and L. Bononi, “A collaborative Internet of Things architecture for smart cities  
 451 and environmental monitoring,” *IEEE Internet of Things Journal*, vol. 5, no. 2, pp. 592–605, 2018.
- 452 [5] S. Dhingra, R.B. Mada, A.H. Gandomi, et al., “Internet of Things Mobile-Air pollution monitoring  
 453 system,” *IEEE Internet of Things Journal*, vol. 6, no. 3, pp. 5577–5584, 2019.
- 454 [6] W. Tang, J. Ren, and Y. Zhang, “Enabling trusted and privacy-preserving healthcare services in social  
 455 media health networks”, *IEEE Transactions on Multimedia*, vol. 21, no. 3, pp. 579–590, 2019.
- 456 [7] W. Tang, J. Ren, K. Deng, et al.,: Secure data aggregation of lightweight E-healthcare IoT devices with  
 457 fair incentives, *IEEE Internet of Things Journal*, accepted, 2019.
- 458 [8] W. Tang, J. Ren, K. Zhang, et al.,: Efficient and privacy-preserving fog-assisted health data sharing  
 459 scheme, *ACM Transactions on Intelligent Systems and Technology*, accepted, 2019.
- 460 [9] F. Alsubaei, S. Shiva, and A. Abuhussein, “Security and privacy in the Internet of Medical Things:  
 461 Taxonomy and risk assessment,” *42<sup>nd</sup> IEEE Conference on Local Computer Networks Workshops*, pp. 112–120,  
 462 2015.
- 463 [10] Federal Communications Commission, “In the Matter of Unlicensed Operation in the TV Broadcast Bands:  
 464 Second Report and Order and Memorandum Opinion and Order”, FCC 08-260, Nov. 2008.
- 465 [11] M. Sharma and A. Sahoo, “Stochastic model based opportunistic channel access in dynamic spectrum  
 466 access networks”, *IEEE Transactions on Mobile Computing*, vol. 13, no. 7, pp. 1625–1639, 2014.
- 467 [12] N. Zhang, H. Liang, N. Chen, et al., “Dynamic spectrum access in multichannel cognitive radio  
 468 networks”, *IEEE Journal on Selected Areas in Communications*, vol. 32, no. 11, pp. 2053–2064, 2014.
- 469 [13] D. Jiang, Y. Wang, C. Yao, et al., “An effective dynamic spectrum access algorithm for multi-hop  
 470 cognitive wireless networks”, *Computer Networks*, vol. 84, pp. 1–16, 2015.

- 471 [14] C. Wang, J. Li, Y. Yang, et al., “Combing solar energy harvesting with wireless charging for hybrid  
472 wireless sensor networks”, *IEEE Transactions on Mobile Computing*, vol. 17, no. 3, pp. 560–576, 2018.
- 473 [15] I. Ahmed, M.M. Butt., C. Psomas, et al., “Survey on energy harvesting wireless communications:  
474 Challenges and opportunities for radio resource allocation”, *Computer Networks*, vol. 88, pp. 234–248, 2015.
- 475 [16] H. Chen, C. Zhai, Y. Li, et al., “Cooperative strategies for wireless-powered communications: An  
476 overview”, *IEEE Wireless Communications*, vol. 25, no. 4, pp. 112–119, 2018.
- 477 [17] K. Tang, R. Shi, and J. Dong, “Throughput analysis of cognitive wireless acoustic sensor networks with  
478 energy harvesting”, *Future Generation Computer Networks*, vol. 86, pp. 1218–1227, 2018.
- 479 [18] Y. Zhang, C. Xu, X. Lin, et al., “Blockchain-based public integrity verification for cloud storage against  
480 procrastinating auditors”, *IEEE Transactions on Cloud Computing*, early access, 2019.
- 481 [19] Mamta and S. Prakash, “An overview of healthcare perspective based security issues in wireless sensor  
482 networks”, *3<sup>rd</sup> International Conference on Computing for Sustainable Global Development*, pp. 870–875, 2016.
- 483 [20] H. Chen, Y. Li, Y. Jiang, et al., “Distributed power splitting for SWIPT in relay interference channels  
484 using game theory”, *IEEE Transactions on Wireless Communications*, vol. 14, no. 1, pp. 410–420, 2015.
- 485 [21] W. Lu, W. Zhao, S. Hu, et al., “OFDM based SWIPT for two-way AF relaying network”, *IEEE Access*,  
486 vol. 6, pp. 73223–73231, 2018.
- 487 [22] L. Shi, Y. Ye, R-Q. Hu, et al., “Energy efficiency maximization for SWIPT enabled two-way DF  
488 relaying”, *IEEE Signal Processing Letters*, vol. 26, no. 5, pp. 755–759, 2019.
- 489 [23] Z. Yan, S. Chen, X. Zhang, et al., “Outage performance analysis of wireless energy harvesting relay-  
490 assisted random underlay cognitive networks”, *IEEE Internet of Things Journal*, vol. 5, no. 4, pp. 2691–2699,  
491 2018.
- 492 [24] S. Aslam, W. Ejaz, and M. Ibnkahla, “Energy and spectral efficient cognitive radio sensor networks for  
493 Internet of Things”, *IEEE Internet of Things Journal*, vol. 5, no. 4, pp. 3220–3233, 2018.
- 494 [25] Y. Zhang, C. Xu, H. Li, et al., “HealthDep: An efficient and secure deduplication scheme for cloud-  
495 assisted eHealth systems”, *IEEE Transactions on Industrial Informatics*, vol. 14, no. 9, pp. 4101–4112, 2018.
- 496 [26] D.S. Gurjar, H.H. Nguyen, and H.D. Tuan, “Wireless information and power transfer for IoT applications  
497 in overlay cognitive radio networks”, *IEEE Internet of Things Journal*, vol. 6, no. 2, pp. 3257–3270, 2019.
- 498 [27] H.A.B. Salameh, S. Almajali, M. Ayyash, et al., “Spectrum assignment in cognitive radio networks for  
499 Internet-of-Things delay-sensitive applications under jamming attacks”, *IEEE Internet of Things Journal*, vol. 5,  
500 no. 3, pp. 1904–1913, 2018.
- 501 [28] Y. Huo, M. Xu, X. Fan, et al., “A novel secure relay selection strategy for energy-harvesting-enabled  
502 Internet of things”, *EURASIP Journal on Wireless Communications and Networking*, vol. 2018, pp. 1–18, 2018.
- 503 [29] Z. Wang, Z. Chen, B. Xia, et al., “Cognitive relay networks with energy harvesting and information  
504 transfer: Design, analysis, and optimization”, *IEEE Transactions on Wireless Communications*, vol. 15, no. 4, pp.  
505 2562–2576, 2016.
- 506 [30] A. Mukherjee, T. Acharya, and M.R.A. Khandaker, “Outage analysis for SWIPT-enabled two-way  
507 cognitive cooperative communications”, *IEEE Transactions on Vehicular Technology*, vol. 67, no. 9, pp. 9032–  
508 9036, 2018.
- 509 [31] C. Zhai, J. Liu, and L. Zheng, “Relay-based spectrum sharing with secondary users powered by wireless  
510 energy harvesting”, *IEEE Transactions on Communications*, vol. 64, no. 5, pp. 1875–1887, 2016.

- 511 [32] C. Tang, G. Pan, and T. Li, "Secrecy outage analysis of underlay cognitive radio unit over Nakagami-m  
512 fading channels", *IEEE Wireless Communications Letters*, vol. 3, no. 6, pp. 609–612, 2014.
- 513 [33] X. Chen, J. Chen, and T. Liu, "Secure transmission in wireless powered massive MIMO relaying systems:  
514 Performance analysis and optimization", *IEEE Transactions on Vehicular Technology*, vol. 65, no. 10, pp. 8025–  
515 8035, 2016.
- 516 [34] Wu. W, B. Wang, Y. Zeng, et al., "Robust secure beamforming for wireless powered full-duplex systems  
517 with self-energy recycling", *IEEE Transactions on Vehicular Technology*, vol. 66, no. 11, pp. 10055–10069, 2017.
- 518 [35] G. Zhang, I. Krikidis, and B. Ottersten, "Full-duplex cooperative cognitive radio with transmit  
519 imperfections", *IEEE Transactions on Wireless Communications*, vol. 12, no. 5, pp. 2498–2511, 2013.
- 520 [36] G. Zhang, H.Z. Jorswieck, and B. Ottersten, "Information and energy cooperation in cognitive radio  
521 networks", *IEEE Transactions on Signal Processing*, vol. 62, no. 9, pp. 2290–2303, 2014.